Title

Timing and significance of pathological features in C9orf72 expansion-associated frontotemporal dementia

Journal

Brain, 139(12)

ISSN

0006-8950

Authors

Vatsavayai, Sarat C
Yoon, Soo Jin
Gardner, Raquel C
et al.

Publication Date

2016-12-01

DOI

10.1093/brain/aww250

Peer reviewed

doi:10.1093/brain/aww250 BRAIN 2016: 139; 3202–3216 | 3202

BRAIN
A JOURNAL OF NEUROLOGY

Timing and significance of pathological features in *C9orf72* expansion-associated frontotemporal dementia

Sarat C. Vatsavayai,[1] Soo Jin Yoon,[2] Raquel C. Gardner,[1] Tania F. Gendron,[3] Jose Norberto S. Vargas,[1] Andrew Trujillo,[1] Mochtar Pribadi,[4] Joanna J. Phillips,[5] Stephanie E. Gaus,[1] John D. Hixson,[6] Paul A. Garcia,[6] Gil D. Rabinovici,[1] Giovanni Coppola,[4] Daniel H. Geschwind,[4] Leonard Petrucelli,[3] Bruce L. Miller[1] and William W. Seeley[1,7]

See Scaber and Talbot (doi:10.1093/aww264) for a scientific commentary on this article.

A GGGGCC repeat expansion in *C9orf72* leads to frontotemporal dementia and/or amyotrophic lateral sclerosis. Diverse pathological features have been identified, and their disease relevance remains much debated. Here, we describe two illuminating patients with frontotemporal dementia due to the *C9orf72* repeat expansion. Case 1 was a 65-year-old female with behavioural variant frontotemporal dementia accompanied by focal degeneration in subgenual anterior cingulate cortex, amygdala, and medial pulvinar thalamus. At autopsy, widespread RNA foci and dipeptide repeat protein inclusions were observed, but TDP-43 pathology was nearly absent, even in degenerating brain regions. Case 2 was a 74-year-old female with atypical frontotemporal dementia–motor neuron disease who underwent temporal lobe resection for epilepsy 5 years prior to her first frontotemporal dementia symptoms. Archival surgical resection tissue contained RNA foci, dipeptide repeat protein inclusions, and loss of nuclear TDP-43 but no TDP-43 inclusions despite florid TDP-43 inclusions at autopsy 8 years after first symptoms. These findings suggest that *C9orf72*-specific phenomena may impact brain structure and function and emerge before first symptoms and TDP-43 aggregation.

1 Memory and Aging Center, Department of Neurology, University of California, San Francisco, CA 94158, USA
2 Department of Neurology, Eulji University Hospital, Eulji University School of Medicine, Daejeon 35233, South Korea
3 Department of Neuroscience, Mayo Clinic Florida, Jacksonville, FL 32224, USA
4 Department of Neurology and Department of Psychiatry, Semel Institute for Neuroscience and Human Behaviour, University of California, Los Angeles, CA 90095, USA
5 Department of Pathology and Department of Neurological Surgery, University of California, San Francisco, CA 94143, USA
6 Epilepsy Center, Department of Neurology, University of California San Francisco, CA 94143, USA
7 Department of Pathology, University of California, San Francisco, CA 94143, USA

Correspondence to: William W. Seeley MD,
UCSF Memory and Aging Center,
675 Nelson Rising Lane,
San Francisco, CA, USA, 94143
E-mail: wseeley@memory.ucsf.edu

Keywords: frontotemporal dementia; protein aggregation; TDP-43

Abbreviations: ALS = amyotrophic lateral sclerosis; FTD = frontotemporal dementia; mPULV = medial pulvinar nucleus of the thalamus; NCI = neuronal cytoplasmic inclusion

Received May 13, 2016. Revised July 21, 2016. Accepted August 16, 2016. Advance Access publication October 22, 2016

Introduction

The *C9orf72* hexanucleotide (GGGGCC) repeat expansion is the most common known genetic cause of frontotemporal dementia (FTD) and amyotrophic lateral sclerosis (ALS) (DeJesus-Hernandez *et al.*, 2011; Renton *et al.*, 2011). The most common FTD syndrome in carriers is the behavioural variant (bvFTD) (Karageorgiou and Miller, 2014), and neuroimaging studies reveal bvFTD-typical atrophy involving anterior cingulate, anterior insula, and frontal and temporal cortices, as well as less typical parietal lobe, medial thalamic, and cerebellar involvement (Mahoney *et al.*, 2012; Sha *et al.*, 2012; Lee *et al.*, 2014). Some carriers with bvFTD, however, exhibit slow progression and/or minimal brain atrophy (Boeve *et al.*, 2012; Khan *et al.*, 2012; Suhonen *et al.*, 2015) despite predictable changes in brain connectivity, suggesting that neuronal dysfunction or disconnection leads to clinical deficits prior to overt neurodegeneration (Lee *et al.*, 2014).

Diverse potential disease mechanisms have been proposed to drive *C9orf72* expansion-related neurodegeneration. These candidates include loss of *C9orf72* gene product function and toxicity through repeat RNA foci and protein aggregation. RNA foci can be composed of sense or antisense repeat mRNA strands (DeJesus-Hernandez *et al.*, 2011; Gendron *et al.*, 2013; Mizielinska *et al.*, 2013) and have been shown to sequester RNA-binding proteins, leading to transcriptome abnormalities (Donnelly *et al.*, 2013; Lee *et al.*, 2013; Mori *et al.*, 2013*a*; Sareen *et al.*, 2013). Expanded repeats also undergo abnormal repeat associated non-ATG (RAN) translation (Zu *et al.*, 2011). In patients, these proteins form stellate cytoplasmic inclusions in degenerate and non-degenerate brain regions (Ash *et al.*, 2013; Mackenzie *et al.*, 2013; Mann *et al.*, 2013; Mori *et al.*, 2013*b*; Zu *et al.*, 2013) and some have been shown to disrupt cellular function and cause toxicity when overexpressed in model systems (Kwon *et al.*, 2014; Mizielinska *et al.*, 2014; Wen *et al.*, 2014; Zhang *et al.*, 2014). Due to the number and complexity of these potential mechanisms, it remains unclear which among them contributes most to disease pathogenesis in patients.

Transactive response DNA-binding protein of 43 kDa (TDP-43; encoded by *TARDBP*) aggregation is a shared feature in frontotemporal lobar degeneration with TDP-43 inclusions (FTLD-TDP) and ALS, with or without the *C9orf72* expansion. Rare carriers show no TDP-43 aggregates or a burden too sparse to classify (Gijselinck *et al.*, 2012; Proudfoot *et al.*, 2014; Baborie *et al.*, 2015). Two recent studies showed that among the five dipeptide repeat proteins only GA (Gly-Ala) in neurites showed a modest correlation with neurodegeneration, whereas TDP-43 burden was closely linked to neurodegeneration severity (Mackenzie *et al.*, 2013, 2015). It remains unclear, however, whether *C9orf72*-associated neurodegeneration can occur in the absence of pathological TDP-43 and in what sequence the various *C9orf72*-associated pathological findings emerge.

Here, we present two patients with *C9orf72*-FTD whose clinical, anatomical, and pathological features shed new light on the timing and significance of *C9orf72*-associated events. Together, these cases reveal that RNA foci and dipeptide repeat protein inclusions can emerge before symptom onset, precede TDP-43 inclusion formation, and accompany clinically significant neurodegeneration in the absence of TDP-43 inclusion pathology.

Materials and methods

Patients and diagnostic neuropathological assessment

Case materials for this study were obtained from the University of California, San Francisco (UCSF) Memory and Aging Center, the UCSF Neurodegenerative Disease Brain Bank, and the Department of Pathology. Patients underwent a clinical history, a neurological examination, and a standard neuropsychological battery. For Case 1, voxel-based morphometry was used to identify the patient's atrophy pattern to matched healthy controls (Supplementary material). Both cases were genotyped for *C9orf72* hexanucleotide repeat expansion using a two-step polymerase chain reaction (PCR)-based procedure as previously described (DeJesus-Hernandez *et al.*, 2011; Sha *et al.*, 2012). Both cases underwent a standard neuropathological assessment of numerous brain regions, which were cut into 8-µm thick formalin-fixed paraffin-embedded tissue sections and subjected to chemical and immunohistochemical stains (Supplementary material). Haematoxylin and eosin stained sections were used to assess regional microvacuolation, astrogliosis, and neuronal loss per routine. Neuronal loss is rated only when it is estimated to exceed 50%. These observations were semiquantitatively rated as – (absent), + (mild), ++ (moderate) and +++ (severe).

Immunohistochemistry

Dipeptide repeat protein and TDP-43 inclusion formation was assessed using immunohistochemistry with the following antibodies: TDP-43 (anti-rabbit, 1:2500, Proteintech), phospho-TDP-43 (pTDP-43, anti-rat, 1:500, courtesy of Prof. Manuela Neumann, University Hospital Tübingen, Germany), and dipeptide repeat protein antibodies, developed by one of the authors (L.P.), that recognize GA (anti-rabbit, 1:20 000), GP (Gly-Pro) (anti-rabbit, 1:20 000), GR (Gly-Arg) (anti-rabbit, 1:5000), PA (Pro-Ala) (anti-rabbit, 1:5000) and PR (Pro-Arg) (anti-rabbit, 1:2000) (Ash *et al.*, 2013; Gendron *et al.*, 2013). Immunostained sections were counterstained with Harris haematoxylin. Inclusion abundance was rated as absent –, scarce (+), mild +, moderate ++, or severe +++. See Supplementary material for additional details.

RNA fluorescence *in situ* hybridization with immunofluorescence

RNA fluorescent *in situ* hybridization and immunofluorescence were applied to single sections to assess the co-occurrence of

RNA foci and dipeptide repeat protein inclusions within individual neurons (Gendron *et al.*, 2013). Oligonucleotide probes were used to identify sense (5'-/Alexa Fluor® 546/-CCCGGCC CCGGCCCC-3', IDT) and anti-sense [5'-/Alexa Fluor® 488/ 2'O-methyl $(GGGGCC)_4$ -3',IDT] RNA foci. After RNA hybridization, tissue sections were subjected to immunofluorescence by incubating with p62 (anti-mouse, 1:200, BD Transduction Laboratories) and with appropriate Alexa Fluor® 647 conjugated secondary antibody (1:200, Life Technologies). Although p62 stains various aggregated proteins, dipeptide repeat protein neuronal cytoplasmic inclusions (NCIs) can be readily identified by their unique stellate morphology and distinguished from other inclusion types. Sections were counterstained with blue fluorescent Nissl to enable visualization of cell types and cell boundaries (NeuroTrace™ 435/ 455, 1:200, Life Technologies). For each brain region, digital image *z*-stacks were captured with a 60× oil immersion objective using a Yokagawa CSU22 spinning disk confocal microscope (Nikon Imaging Center, UCSF) to quantify the proportion of individual neurons containing one, two, or more than two pathological features.

Results

Two patients provide rare windows into *C9orf72* pathogenesis

Case 1 was a 65-year-old right-handed female who at age 53 years developed new anxiety about being left home alone. At age 54, she had an uncharacteristic verbal altercation with a store clerk. Over the following 2 years, her libido declined, she binge drank, and she became verbally aggressive even toward young children. She developed recurring spells of prolonged pacing (up to 14 h), during which she stared and muttered. She drove her car around her block for hours at a time. At age 57, she became incontinent of urine and gained weight from overeating. Bilateral rest and postural hand tremors, forgetfulness, word-finding difficulty, and compulsivity emerged. By age 59, she was apathetic and mildly disinhibited, with blunted emotions and little regard for personal hygiene. She had developed episodes of agitation and occasional days during which she was surprisingly lucid. Three relatives, including a parent and sibling, had prominent psychiatric histories with severe mood disorders, including depression and bipolar disorder, but none had a history of dementia or motor neuron disease. On examination, she had flat affect, violated interpersonal boundaries, and acted impulsively. There was mild parkinsonism, likely due to quetiapine, and diffuse hyperreflexia. Her Mini-Mental State Examination score was 26/30. A complete neuropsychological battery revealed mild-to-moderate impairments in visual more than verbal memory, naming, and visuospatial skills, and severe executive deficits. A routine clinical MRI obtained at age 59 revealed normal findings. An inpatient EEG revealed slowing and loss of background elements in both hemispheres with an occasional 6–7 Hz posteriorly predominant rhythm bilaterally but no epileptiform activity. Her clinical diagnosis was bvFTD. She continued to progress slowly and developed panic attack-like spells, lasting hours, one to two times per week. At age 65, she fell, fractured her hip, and entered hospice care for 2 weeks prior to her death. Genetic analysis revealed a *C9orf72* hexanucleotide repeat expansion.

At autopsy, the fresh brain weighed 1044 g and showed little gross atrophy (Fig. 1B). Microscopic examination, performed blind to the patient's genetic status, revealed a conspicuous lack of neurodegenerative changes, such as microvacuolation and gliosis (Table 1). Neuronal loss was deemed absent or too mild to visually quantify (i.e. $<50\%$) throughout. Exceptions included the subgenual anterior cingulate cortex, amygdala, and, most prominently, the medial pulvinar nucleus of the thalamus (mPULV). Motivated by these focal neurodegenerative changes, we returned to the patient's research MRI scan, obtained at age 60 (5 years prior to death), to compare Case 1's T_1-weighted image to 25 age-matched controls, using voxel-based morphometry. Consistent with the post-mortem findings, the subgenual anterior cingulate cortex and mPULV stood out among the few regions showing antemortem atrophy (Fig. 1A). TDP-43 immunohistochemistry was remarkable for the general lack of TDP-43 inclusions (Table 1); no more than one to two wispy threads of TDP-43 were seen throughout the subgenual anterior cingulate cortex and medial pulvinar thalamus, the most degenerate regions. Due to the scarcity of TDP-43 lesions, the pattern could not be classified as a specific FTLD-TDP subtype. Ubiquitin and p62 immunohistochemistry, however, revealed abundant stellate NCIs suggestive of a *C9orf72* expansion. Amyloid-β and α-synuclein immunohistochemistry studies were unrevealing, and tau immunohistochemistry showed Braak stage 3 neurofibrillary degeneration.

Case 2 was a 74-year-old ambidextrous female with a longstanding seizure disorder who presented at age 69 for progressive cognitive and behavioural disturbance. In childhood, she fell from a horse, suffered a traumatic brain injury, and remained unresponsive in the hospital for 3 days. Complex partial seizures began at age 30 years and were treated with phenytoin. Four years later, she developed generalized tonic-clonic seizures and was treated with multiple medications with limited success. At age 50, she became seizure-free for 6 years on lamotrigine monotherapy. At age 56, complex partial seizures recurred and proved refractory. At age 61, presurgical neuropsychological assessment revealed impaired verbal and visual memory and impaired figure copying. An intracarotid amobarbital test confirmed left hemisphere language lateralization. MRI (Fig. 1C and D) showed left anteromesial temporal and hippocampal atrophy, as well as mild dorsal frontoparietal atrophy, and inpatient EEG telemetry suggested a left temporal lobe seizure focus. She underwent a left anterior temporal lobectomy with amygdalohippocampectomy. Surgical pathology reports indicated maximal astrogliosis in the hippocampus. Language difficulties

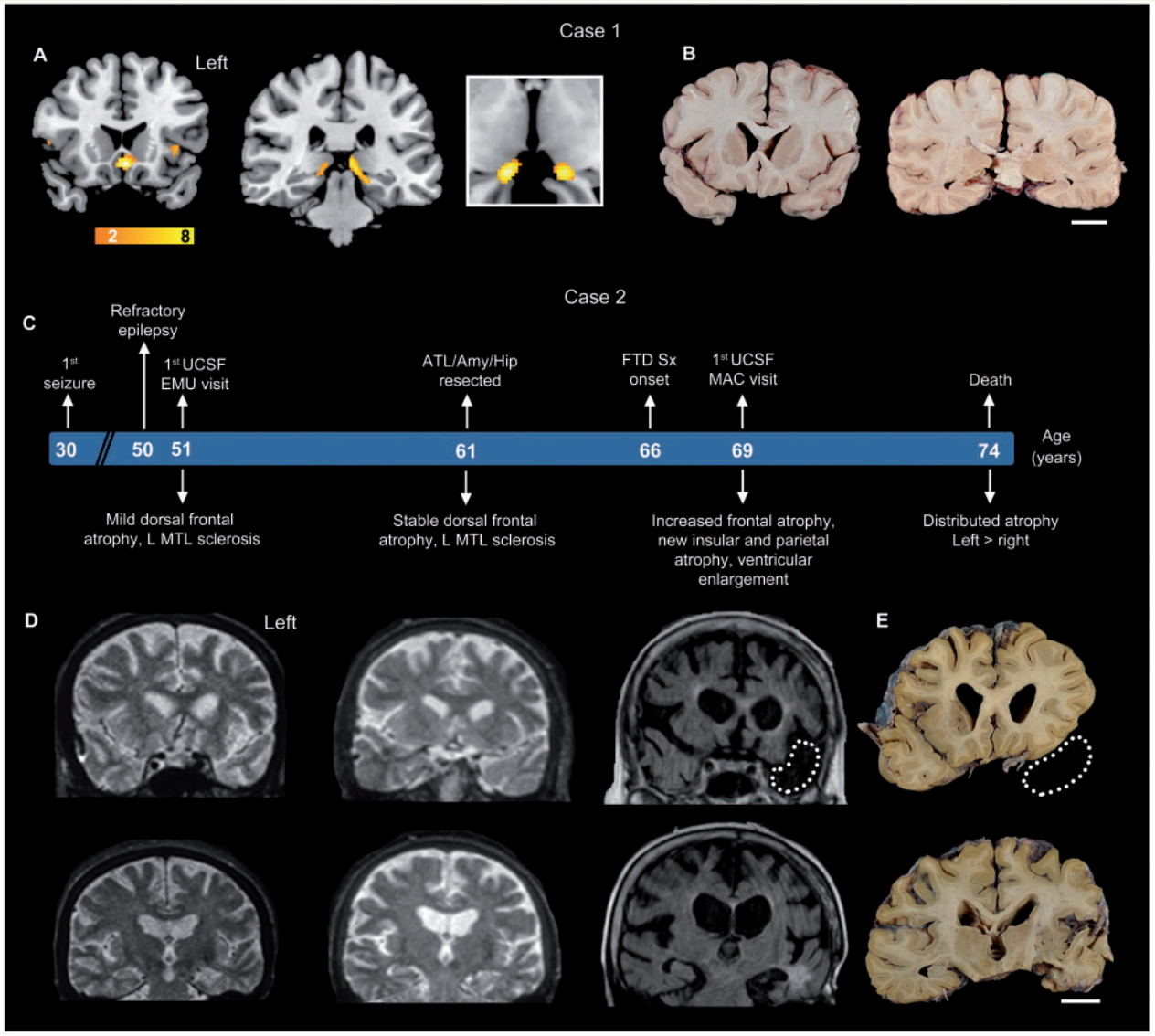

Figure 1 Two uniquely illustrative patients with *C9orf72* FTD. (**A**) Case 1. Voxel-based morphometry showed mild, focal atrophy in subgenual anterior cingulate cortex, anterior insula and medial pulvinar nucleus of thalamus (yellow-orange colour scale represents *t*-statistics in the Case 1 < controls). Cropped image shows axial view of atrophy observed in bilateral medial pulvinar thalamus. (**B**) Case 1. Fixed coronal brain slabs show a striking absence of cortical thinning or ventricular enlargement but moderate bilateral medial thalamic atrophy. (**C–E**) Case 2. Schematic shows clinical milestones above and anatomical features below the patient's age timeline. MRI 15 years prior to FTD symptom onset revealed mild frontal atrophy, which remained stable over a 10-year follow-up interval. Three years after clinical onset, brain MRI showed more pronounced brain atrophy and ventricular enlargement. Dotted lines represent the surgical resection cavity in the MRI and in the corresponding post-mortem brain slab. Scale bars for Cases 1 and 2 = 2 cm. EMU = Epilepsy Monitoring Unit; MAC = Memory and Aging Center; UCSF = University of California, San Francisco; L MTL = left middle temporal lobe.

emerged immediately following surgery, but she recovered almost completely before discharge. Her usual seizures remitted and did not return.

Beginning around age 66, she showed gradually increasing apathy, with poor initiative and disinterest in her usual activities. She developed memory, word-finding and visuospatial difficulties, occasionally getting lost in familiar environments and struggling to recognize and name faces. At age 67, she began to complain about 'nocturnal events' characterized by sudden 'urinary urges', 'cold feelings', 'migraine-like' headaches, and moaning, followed by a feeling of morning limb soreness and anorexia. She remained aware throughout the events, which lasted 10 to 30 s and involved no stereotypic movements or unusual behaviours. She was treated with multiple antiepileptic drugs but continued to have three to five episodes per month. Inpatient video-EEG monitoring revealed no epileptiform discharges during a typical nocturnal spell. By age 68, she had become housebound with increasing anxiety and depression. By her first UCSF Memory and Aging Center visit at age 69, she had developed mental rigidity and compulsively played solitaire, Sudoku, and word games throughout the day. She

Table 1 A summary of neuropathological findings from Case 1

Brain region	Side	Vacuolation	Gliosis	TDP-43	GA	GP	GR	PA	PR
aMCC	R	–	–	(+)	+ + +	+ +	+ +	(+)	(+)
sACC	R	+ +	+ +	–	+ + +	+	+ +	(+)	(+)
preCG	R	–	–	–	+ +	+	+ +	(+)	(+)
postCG	R	–	–	–	+ +	+	+ +	(+)	(+)
ITG	R	–	–	–	+ + +	+ +	+ +	(+)	(+)
Calc ctx	R	–	–	–	+ +	+	+	–	–
ERC	R	–	–	–	+ + +	+ +	+ +	(+)	(+)
Hip-DG	R		–	–	+	+	+ +	(+)	–
Hip-CA3–4	R		–	–	+ +	+ + +	+ +	(+)	(+)
Hip-CA2	R		–	–	+ +	+ + +	+ +	–	(+)
Hip-CA1-subiculum	R		–	–	+ +	+ + +	+ + +	(+)	(+)
Amygdala	R		+ +	–	+ + +	+ + +	+	(+)	(+)
Thalamus (mPULV)	R		+ + +	–	+ + +	+ + +	+ + +	(+)	(+)
vSTR	R		–	(+)	+	+	+	–	(+)
Cerebellar cortex	L		–	–	+ + +	+ + +	+ + +	–	(+)
Cerebellum – DN	L		–	–	+	+	+	–	–
Inferior olive	B		–	–	+	+	+	–	–
SC - cervical AHCs	B		–	–	–	+	–	–	–
SC - thoracic AHCs	B		–	–	+	+	–	–	–
SC - lumbar AHCs	B		–	–	–	+	–	–	–
SC - sacral AHCs	B		–	–	+	+	–	–	–

Neurodegenerative changes and cellular inclusions were assessed using a semi-quantitative rating system. Vacuolation and gliosis were rated as – (absent), + (mild), + + (moderate) and + + + (severe). TDP-43 NCIs and dipeptide repeat protein NCIs were rated as – (absent or 1–2 inclusions total per section), (+) (scarce), + (mild), + + (moderate) and + + + (severe). Vacuolation was assessed only in cortical regions. DN = dystrophic neurites; aMCC = anterior midcingulate cortex; sACC = subgenual anterior cingulate cortex; preCG = precentral gyrus; postCG = postcentral gyrus; ITG = inferior temporal gyrus; Calc ctx = calcarine cortex; ERC = entorhinal cortex; Hip = hippocampus; vSTR = ventral striatum; SC = spinal cord; AHCs = anterior horn cells; L = left; R = right; B = bilateral.

was socially detached but remained warm and empathic toward her husband. She was disorganized, with difficulties problem-solving and multitasking. Idiosyncratic eating habits emerged, including a general distaste for food, but she gained perhaps 30 lb over 3 months. She had become increasingly reliant on her husband, could no longer manage home finances, and needed help tracking her medications. Her parents died in their 60s due to cardiovascular disease, and none of her three surviving first degree relatives was known to suffer from a neurodegenerative disease. On examination, affect was dysregulated, alternating between melancholia and anxious or childish giggles. She waved and smiled at strangers and patients in the hospital setting. She lacked insight into her deficits. Spontaneous speech was fluent though somewhat empty, and she occasionally used non-specific descriptor words like 'that' and 'those things'. Confrontation naming was good, and she retained substantial semantic knowledge, although she spelled irregular words phonetically. She could repeat short but not long phrases. She showed mild ideomotor apraxia. Cranial nerves were unremarkable. There was a mild high frequency postural hand tremor. Muscle bulk, tone, and power were normal and no fasciculations were observed. Deep tendon reflexes were normal. Gait was unremarkable. The Mini-Mental State Examination score was 23/30. A complete neuropsychological battery revealed only mild verbal and moderate visual memory deficits, moderate anomia, and severe deficits in working memory and executive functions. Brain MRI showed cerebral atrophy most prominently affecting the posterior parietal and temporal structures and thalamus, as well as the frontal and anterior temporal lobes (Fig. 1C and D). By age 72, she had developed severe motor speech impairment. She could barely phonate and had stopped writing. There was no spontaneous speech, and attempts to speak had a strained and spastic quality. She could generate no more than three or four repeated syllables and could not hold a note, but she could follow complex and multi-step commands, perform simple mental arithmetic, and communicate answers with her fingers. Her facial affect was imitative, but there were no face or tongue fasciculations. Limb power was full. Muscle tone was mildly increased bilaterally and there was mild dystonia in both hands. She had a manual grasp response bilaterally. Repetitive hand and foot movements were slow with normal amplitude. Posture was upright but with a significant anterocollis. Gait was unremarkable. Her clinical diagnosis was atypical FTD-MND, with mild upper motor neuron disease features. Case 2's symptoms progressed, and she died at age 74.

At autopsy, the fresh brain weighed 980 g, and there was moderate atrophy in frontal, parietal, striatal and thalamic regions, worse on the left, with moderate ventricular enlargement (Fig. 1E). The substantia nigra showed moderate depigmentation. Microscopically, there was mild frontal and severe thalamic neurodegeneration (Table 2).

Table 2 Neuropathological findings in preclinical and post-mortem brain regions from Case 2

Brain region	Side	Vacuolation	Gliosis	TDP-43	GA	GP	GR	PA	PR
Surgical block									
Lateral temporal cortex	L	–	+	–	+	+	+	ND	ND
Temporal pole	L	NR	NR	–	+	+	ND	ND	ND
Hippocampus	L	NR	NR	–	ND	ND	ND	–	–
Amygdala	L	NR	NR	–	ND	ND	ND	ND	ND
Post-mortem tissue									
aMCC	L	+	–	+ +	+ +	+	+	(+)	–
sACC	L	+	+	+ +	+ +	+	+	(+)	(+)
preCG	R	+	+	+	+ +	+	+	–	–
postCG	R	+	–	+	+ +	+	+	–	–
ITG	R	–	–	+	+ +	+	+	(+)	(+)
Calc ctx	R	–	–	–	+ +	+	+	(+)	–
ERC	R	+	–	+	+ + +	+	+	(+)	–
Hip-DG	R		–	–	+ + +	+	+	(+)	–
Hip-CA3–4	R		–	–	+	+	+	(+)	–
Hip-CA2	R		–	–	+	+	+	–	–
Hip-CA1-subiculum	R		–	+	+	+	+	–	–
Amygdala	R		–	+	+	+	+	(+)	–
Thalamus (mPULV)	R		+ + +	+	+ +	+	+	–	–
vSTR	L		–	+ +	+	+	+	–	–
Cerebellar cortex	L		–	–	+ +	+ + +	+ +	–	–
Cerebellum - DN	L		–	–	+	+	–	–	–
Inferior olive	B		–	–	–	+	–	–	–
SC - cervical AHCs	B		+	–	–	–	–	(+)	–

Neurodegenerative changes and cellular inclusions were assessed using a semi-quantitative rating system. Vacuolation and gliosis were rated as were rated as – (absent), + (mild), + + (moderate) and + + + (severe). TDP-43 NCIs and dipeptide repeat protein NCIs were rated as – (absent or 1–2 inclusions total per section), (+) (scarce), + (mild), + + (moderate) and + + + (severe). Vacuolation was assessed only in cortical regions. DN = dystrophic neurites; ND = not determined; NR = sections not suitable for rating; aMCC = anterior midcingulate cortex; sACC = subgenual anterior cingulate cortex; preCG = precentral gyrus; postCG = postcentral gyrus; ITG = inferior temporal gyrus; Calc ctx = calcarine cortex; ERC = entorhinal cortex; Hip = hippocampus; vSTR = ventral striatum; SC = spinal cord; AHCs = anterior horn cells; L = left; R = right; B = bilateral.

Immunohistochemistry demonstrated diffuse/granular TDP-43 NCIs in all cortical layers and scattered short dystrophic neurites, consistent with FTLD-TDP, Type B. p62 immunohistochemistry revealed stellate NCIs suggestive of a *C9orf72* expansion, which was confirmed through genetic analysis of a frozen brain sample taken at autopsy. Immunostains revealed no amyloid-β deposits and a Braak neurofibrillary tangle stage of 4. Scattered Lewy bodies and Lewy neurites were seen only in the right amygdala.

Neurodegeneration in *C9orf72* FTD can occur in the absence of TDP-43 aggregation (Case 1)

In *C9orf72* expansion disease, TDP-43 inclusions are a nearly universal feature, and previous studies have correlated TDP-43 inclusion burden with neurodegeneration (Mackenzie *et al.*, 2013, 2015). With rare exceptions (Gijselinck *et al.*, 2012), patients show well-developed TDP-43 NCIs that are intermingled with dipeptide repeat protein inclusions and RNA foci, making it difficult to disentangle the relationship of each inclusion type to neurodegeneration where multiple types are present. Case 1, having a focal degenerative pattern with scarce TDP-43 pathology, presented an opportunity to clarify the relationship between *C9orf72*-associated pathological findings and neurodegeneration severity. We therefore undertook a more extensive analysis that included TDP-43 inclusions, RAN-translated dipeptide repeat protein inclusions, and sense and antisense RNA foci (Figs 2 and 3, and Table 1). Across brain regions, TDP-43 staining showed a predominantly normal nuclear pattern, with scarce to absent threads and NCIs in degenerate and non-degenerate regions alike. Even in medial pulvinar thalamus, which showed the most severe antemortem magnetic resonance atrophy and post-mortem neurodegeneration, TDP-43 inclusions were all but absent. These Case 1 findings show that neurodegeneration can occur even when TDP-43 aggregation is scarce to absent.

Dipeptide inclusions and RNA foci are distributed throughout degenerate and non-degenerate brain regions

All five dipeptide repeat protein NCI subtypes were observed in Cases 1 and 2. These inclusions exhibited a characteristic stellate or dot-like morphology, and all five dipeptide repeat protein subtypes often co-occurred in the same brain region (Fig. 2, Tables 1 and 2). GA, GP, and GR NCIs predominated, whereas PA and PR NCIs were rare (Tables 1 and 2), consistent with previous findings

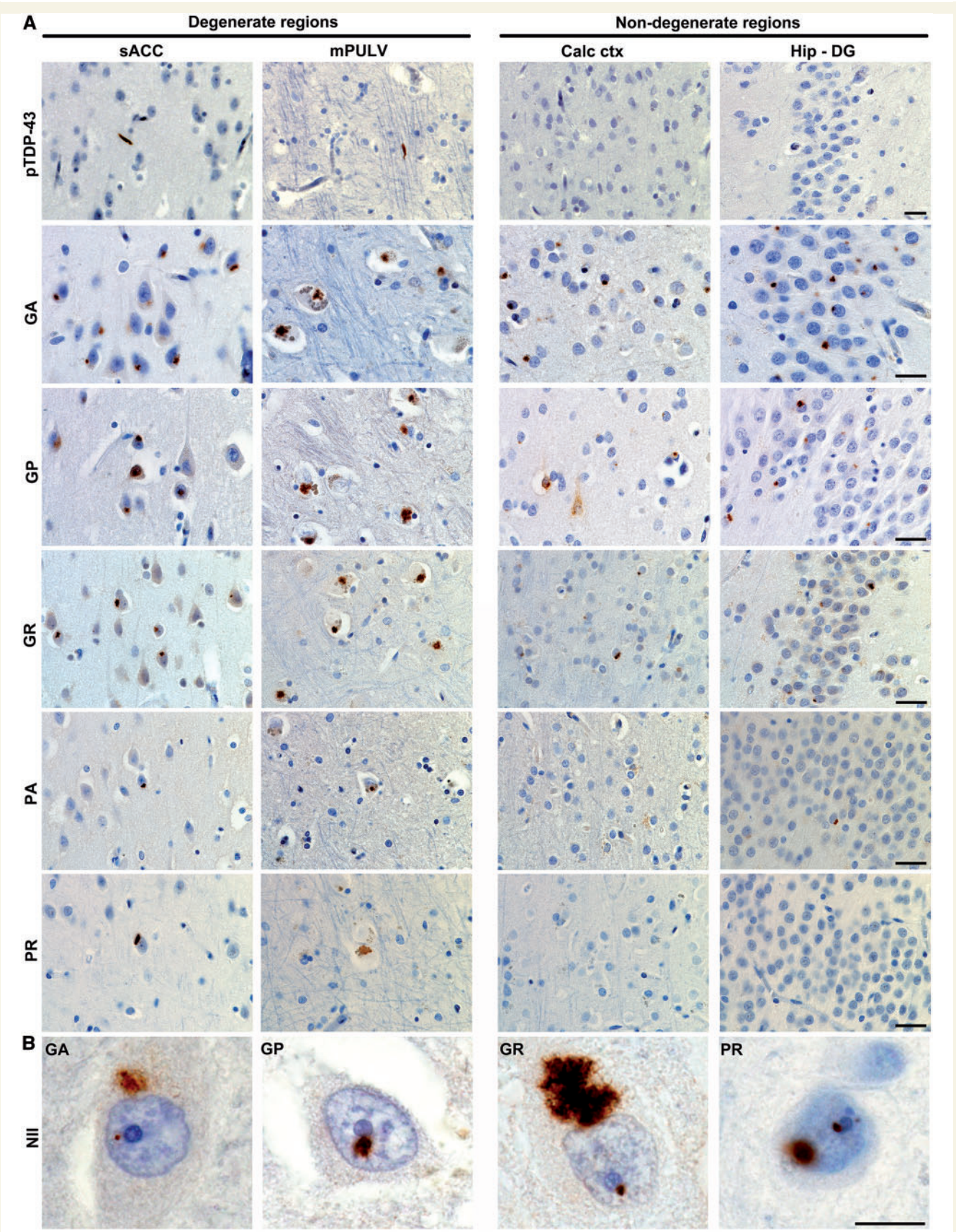

Figure 2 Abundant dipeptide repeat protein inclusions in the near absence of TDP-43 aggregation (Case 1). (**A**) Representative images show dipeptide repeat protein inclusions in degenerate and non-degenerate brain regions. pTDP-43 immunostaining showed sparse to absent TDP-43 inclusions. GA, GP and GR NCI were abundant whereas PA and PR aggregates were sparse to absent. Scale bars = 25 μm. (**B**) Occasional neuronal intranuclear inclusions (NII) were also observed, often adjacent to the nucleolus, for all dipeptide repeat proteins except for PA. Scale bar = 10 μm. sACC = subgenual anterior cingulate cortex; Calc ctx = calcarine cortex; Hip-DG = dentate gyrus of hippocampus.

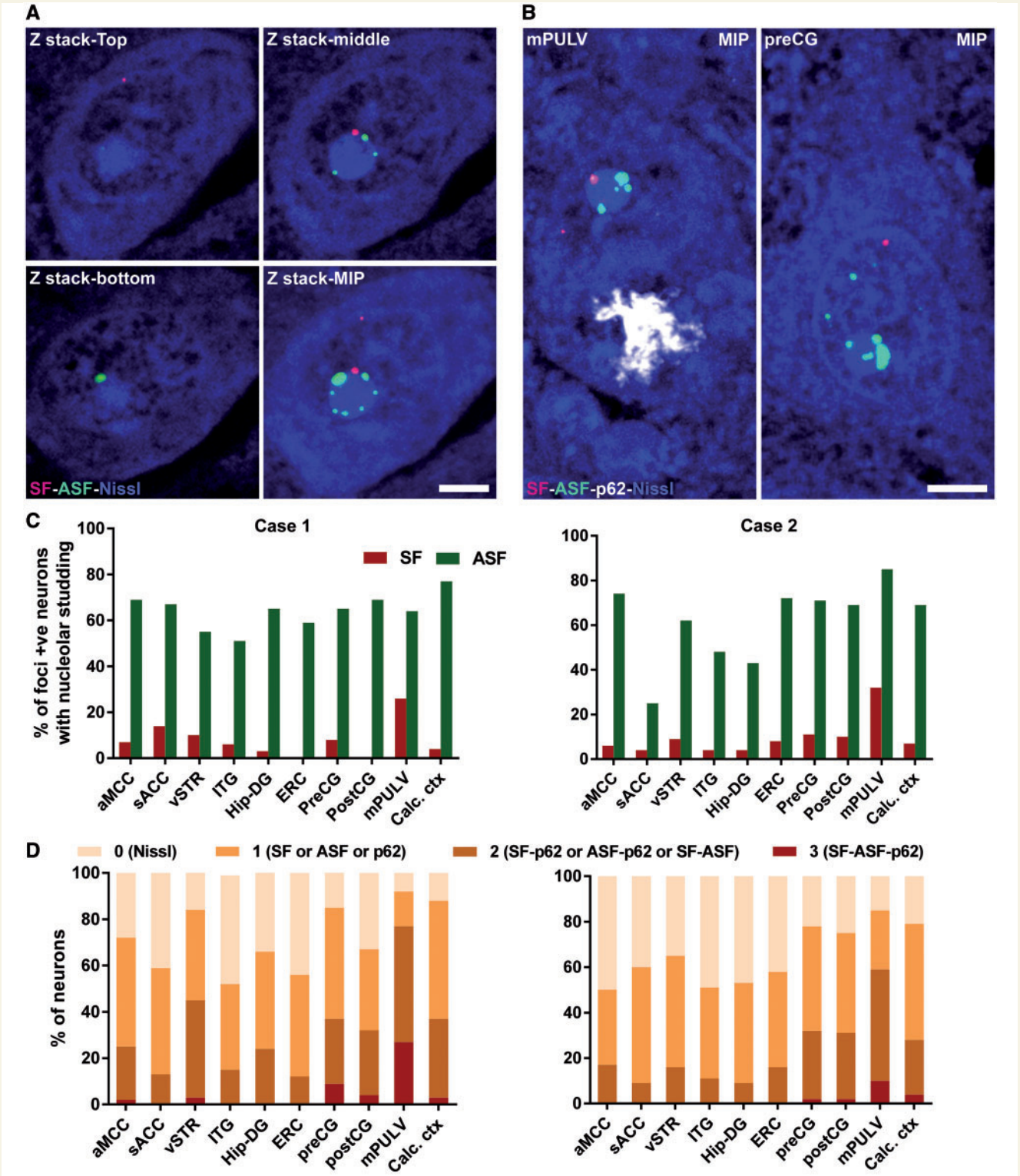

Figure 3 Single neurons in degenerate brain regions harbour multiple *C9orf72*-associated inclusions. (**A**) Representative individual z-stack and maximum intensity projection (MIP) images from a single mPULV thalamic neuron show perinucleolar RNA foci. (**B**) MIP images from the mPULV and preCG show representative individual neurons with multiple types of inclusions. Scale bar = 5 μm for **A** and **B**. (**C**) Bar graphs depict the proportion of neurons in which at least one RNA focus directly abuts the nucleolus; this 'nucleolar studding' was more frequent for antisense than sense foci. (**D**) Stacked bars show the proportion of neurons harbouring 0, 1, 2, or 3 *C9orf72*-specific inclusion types across regions for Cases 1 and 2. In both patients, mPULV stood out as having the fewest neurons with no inclusions and the most with 2 or 3 inclusions. Direct statistical comparison between mPULV and non-PULV regions showed higher pathological multiplicity in mPULV ($P < 0.001$, see 'Results' section). aMCC = anterior midcingulate cortex; preCG = precentral gyrus; postCG = postcentral gyrus; ITG = inferior temporal gyrus; ERC = entorhinal cortex; vSTR = ventral striatum; sACC = subgenual anterior cingulate cortex; Calc ctx = calcarine cortex; Hip-DG = dentate gyrus of hippocampus.

(Ash *et al.*, 2013; Mackenzie *et al.*, 2013; Mann *et al.*, 2013; Mori *et al.*, 2013*b*; Zu *et al.*, 2013). Overall, especially in the cerebral cortex, GA, GP, and GR NCIs showed a widespread regional distribution in both cases, including degenerate and non-degenerate brain regions (Fig. 2, Tables 1 and 2). Along with typical stellate NCIs, dipeptide repeat protein staining showed additional patterns, including neuronal intranuclear inclusions, diffuse cytoplasmic staining, and dendritic staining (Fig. 2B and Supplementary Fig. 1).

Like dipeptide repeat protein NCIs, sense and antisense RNA foci were present within degenerate and non-degenerate brain regions in both cases (Supplementary Table 1). RNA foci proved more difficult to quantify due to their small size and high frequency even within single neuron. Overall, the findings described in this section suggest a poor fit between the regional patterns of neurodegeneration and the distribution of dipeptide repeat protein NCIs or RNA foci, suggesting that neither dipeptide repeat protein inclusions nor RNA foci are sufficient to produce regional neurodegeneration wherever they are found.

Individual neurons in medial pulvinar thalamus harbour multiple *C9orf72*-specific inclusions

If TDP-43 NCIs are not necessary for regional neurodegeneration (Case 1), and dipeptide repeat protein NCIs and RNA foci are not sufficient to produce regional degeneration (Cases 1 and 2), what factors determine the graded neurodegeneration landscape in patients with *C9orf72* disease? Limited information is available regarding how often individual neurons contain multiple *C9orf72*-specific pathological features (Gendron *et al.*, 2013; Mizielinska *et al.*, 2013). To address this question for Cases 1 and 2, we combined RNA fluorescent *in situ* hybridization for sense and antisense foci with immunofluorescence for p62, which can be used to identify dipeptide repeat protein NCIs based on their unique stellate morphology.

Neurons with sense foci were slightly more abundant than those with antisense foci, although neurons often harboured both sense and antisense foci (Supplementary Table 1). Foci were often found in the nucleus and rarely in the cytoplasm. Nuclear foci were located either in the nucleoplasm, abutting the nucleolus, or both (Fig. 3A and B and Supplementary Fig. 2). Unexpectedly, RNA foci were often seen in multiples studding the rim of the nucleolus; this pattern was particularly frequent among antisense foci (Fig. 3C). This subcellular distribution is perhaps made more evident when counterstaining for Nissl, which produces a densely stained nucleolus. Foci associated with the nucleolus were often larger than those in the nucleoplasm. In both cases, the proportion of antisense foci-containing neurons in which at least one focus abutted the nucleolus varied according to brain region, ranging from 25% to 85% of neurons (Fig. 3C). Neurons containing sense foci far less often included a perinucleolar sense focus (0–32%). Interestingly, perinucleolar sense foci were more frequent in mPULV in both Cases 1 and 2 (26% and 32%) compared to other regions.

To estimate how often individual neurons contained multiple distinct *C9orf72* expansion-specific inclusions, we characterized neurons as containing one, two, or more than two inclusion types. By considering sense foci, antisense foci, and dipeptide repeat protein inclusions simultaneously, we found that, across diverse brain regions, 53–92% (Case 1) and 50–85% (Case 2) of individual neurons contained at least one inclusion type (Fig. 3D and Supplementary Table 1). Strikingly, the mPULV stood out in Case 1 as the region where almost no neurons were free of inclusions and nearly 27% of neurons showed all three inclusion types (Fig. 3D). To assess this observation more formally, we grouped brain regions assessed as mPULV or non-mPULV and compared the distribution of inclusion multiplicity within these groups. The mPULV showed a higher degree of multiplicity than non-mPULV regions (Mann-Whitney $U = 30\,776$ for Case 1 and 39 184 for Case 2, $P < 0.001$).

C9orf72-associated inclusions can occur prior to symptom onset

Because FTD has a relatively low prevalence, opportunities to examine brain tissue from individuals with preclinical FTD are scarce (Miki *et al.*, 2014). Case 2 presented an even more extraordinary opportunity to compare brain magnetic resonance images and brain tissues that represent the presymptomatic and symptomatic disease stages in the same *C9orf72* expansion-carrying individual. Her post-mortem brain showed pathological findings typical of the mutation. All five RAN-translated dipeptide repeat protein inclusions, sense and antisense RNA foci, and TDP-43 NCI and dystrophic neurites were widely distributed (Table 2 and Fig. 4).

As treatment for her refractory epilepsy, Case 2 underwent a left anteromesial temporal lobe resection 5 years prior to FTD symptom onset and 13 years before death (Fig. 4A). Archival resected tissue specimens included lateral temporal cortex, temporal pole, hippocampus and amygdala. Within these regions, we observed GA, GP and GR dipeptide inclusions and sense and antisense RNA foci, indicating that these pathological features emerge during the presymptomatic stage of *C9orf72* expansion-related FTD (Table 2, Fig. 4 and Supplementary Fig. 3). The dipeptide repeat protein inclusions were abundant throughout (Fig. 5B–D), and occasional neurons with diffuse GP labelling were also observed (Fig. 5C). PA and PR dipeptide inclusions were absent in surgically resected hippocampus, and considering the paucity of PA and PR inclusions in post-mortem brain we did no further testing for PA or PR in the remaining tissue specimens. Sense and antisense RNA foci were observed in the resected left temporal pole and hippocampus (Fig. 4 and Supplementary Fig. 3)

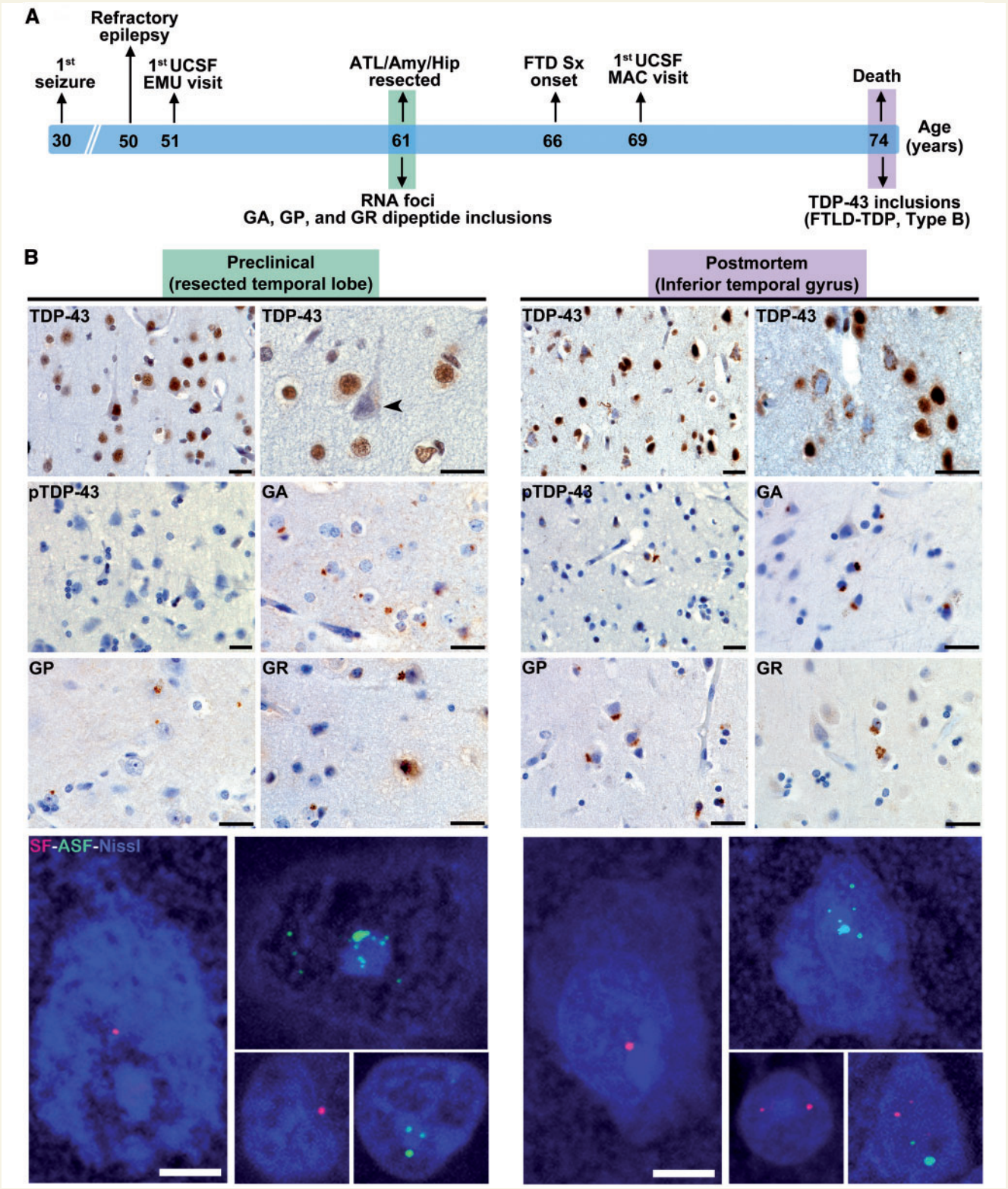

Figure 4 ***C9orf72*-specific pathological inclusions precede TDP-43 aggregation.** (**A**) Schematic shows clinical milestones (*above*) and microscopic neuropathological features (*below*) in reference to the patient's age timeline. (**B**) The resected left anterior temporal lobe represents the preclinical stage and is compared to post-mortem tissue from the contralateral anterior inferior temporal lobe. In the resected left temporal lobe, TDP-43 immunostaining revealed only a single NCI and no dystrophic neurites (Fig. 5). Intriguingly, numerous neurons lacking normal nuclear TDP-43 were observed in the apparent absence of a TDP-43 inclusion (arrowhead). These findings stand in contrast to the well-developed FTLD-TDP, type B, seen at autopsy. RAN-translated GA, GP and GR inclusions, as well as sense and antisense RNA foci, were conspicuous in both surgically resected tissue and post-mortem brain. Images with RNA foci are maximum intensity projections of a z-stack image to show the approximate abundance of foci within individual nuclei. Scale bars = 25 μm for bright field and 5 μm for fluorescent images. FTLD = frontotemporal lobar degeneration; DN = dystrophic neurites; RAN = repeat associated non-ATG; MAC = Memory and Aging Center; UCSF = University of California, San Francisco; ATL = anterior temporal lobe; EMU = Epilepsy Monitoring Unit.

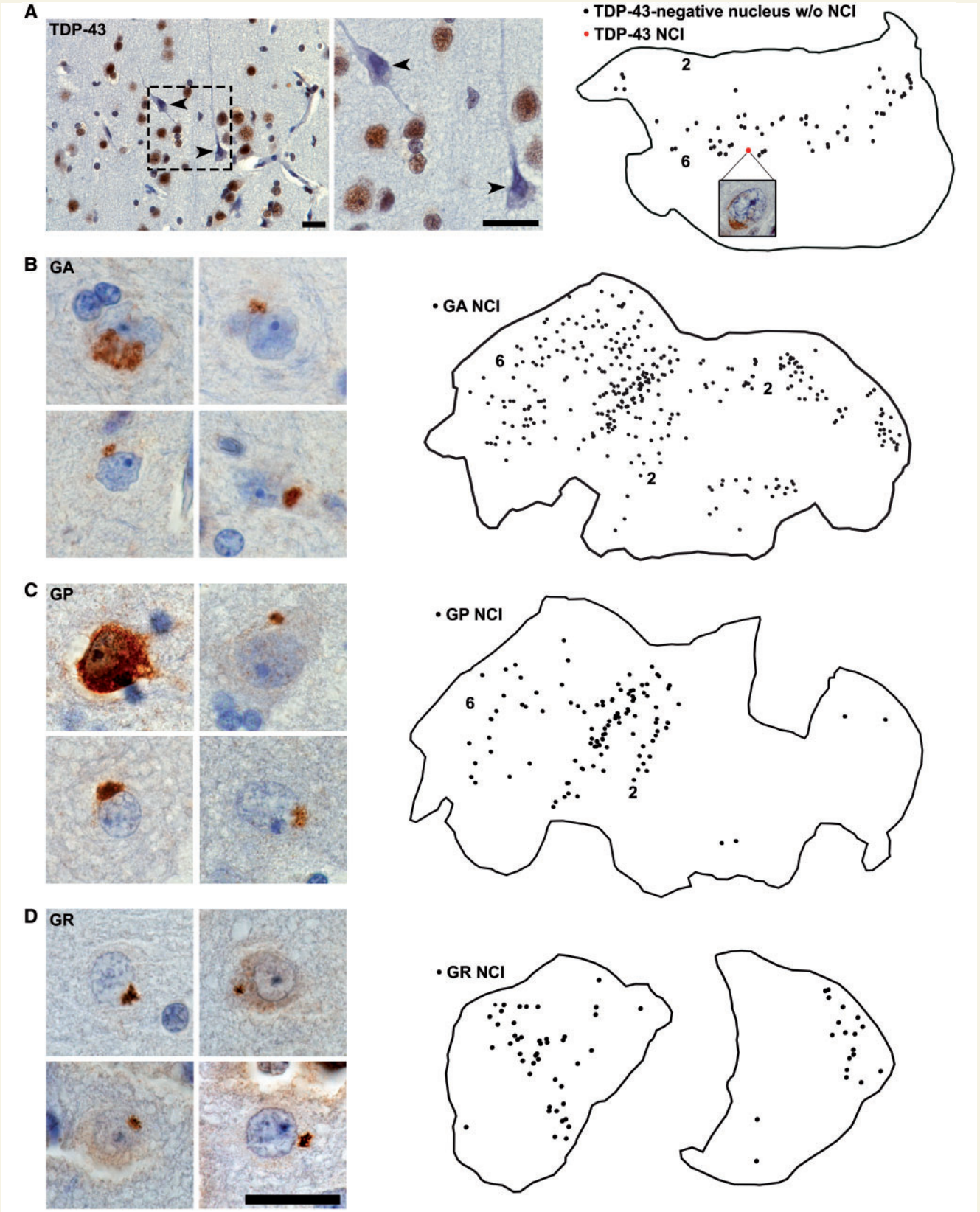

Figure 5 Distribution of *C9orf72* expansion-associated inclusions in Case 2's preclinically resected lateral temporal lobe. Tissues sections were traced and subjected to exhaustive mapping at 60 × magnification. (**A**) TDP-43 immunohistochemistry revealed numerous neurons lacking nuclear staining despite the absence of an apparent TDP-43 inclusion (arrowheads in photomicrographs and black dots in map). These neurons were most abundant in deep cortical layers. Only one neuron with a TDP-43 cytoplasmic inclusion was observed (red dot and map inset). (**B–D**) GA, GP and GR dipeptide repeat protein NCI were abundant. Numbers 2 and 6 denote cortical layers within section tracings. Scale bar = 25 μm.

In contrast to the *C9orf72*-specific phenomena, TDP-43 and pTDP-43 immunohistochemistry uncovered essentially no TDP-43 inclusions in the surgical resection specimens (Table 2). To supplement our routine assessments, we performed exhaustive mapping across traced tissue sections from resected lateral temporal cortex. This process revealed only a single neuron with a TDP-43 NCI (Fig. 5A). Post-mortem brain tissue from regions adjacent and contralateral to the resection cavity, however, showed well-developed FTLD-TDP, type B, suggesting that TDP-43 aggregation emerges later in the disease course than *C9orf72* expansion-specific phenomena (Fig. 4B). For Case 2, it remains uncertain, however, when TDP-43 aggregation emerged with respect to FTD symptom onset.

Interestingly, in the surgical specimens, we observed multiple neurons without nuclear TDP-43 staining (Figs 4B and 5A and Supplementary Fig. 4). These neurons lacked TDP-43 inclusions but often had a shrunken, atrophic appearance and were predominantly located in cortical layer 5–6. Neurons with a similar TDP-43 phenotype were also present in the post-mortem brain from Case 2, where they were less frequent than TDP-43 NCI-containing neurons (Supplementary Fig. 4). Because relatively few neurons lacking nuclear TDP-43 were observed, we could not perform a quantitative study of associated *C9orf72*-specific inclusions. Sections fluorescently co-stained for sense foci, TDP-43, p62, and Nissl revealed no clear cut association, however, between neurons lacking nuclear TDP-43 and other *C9orf72*-associated inclusions. In Case 1, similar neurons lacking nuclear TDP-43 were not observed in the most degenerate brain regions, including subgenual anterior cingulate cortex, mPULV and amygdala. This novel observation raises the possibility that abnormal TDP-43 expression or localization represents an early feature in *C9orf72* disease, occurring prior to frank TDP-43 inclusion formation.

Discussion

Experimental models of *C9orf72* hexanucleotide repeat expansion disease have begun to compare the pathogenicity of the various phenomena observed in human brain and spinal cord tissues. Human post-mortem studies play essential roles in (i) establishing disease features for models to emulate; (ii) grounding and validating unforeseen conclusions drawn from model systems; and (iii) addressing key questions that model systems, by their nature, cannot examine. Here, we describe two patients who provide new insights regarding the pathogenicity and timing of *C9orf72*-related events. Although these patients are unusual and may not generalize to all *C9orf72* disease, their neuropathological features and circumstances provide unprecedented opportunities to dissect apart contributions of the multiple pathological processes that comingle in most cross-sectional post-mortem studies of late stage *C9orf72*-FTD/ALS. Case 1 showed focal degeneration within structures that lacked TDP-43 inclusions but harboured a multiplicity of *C9orf72*-specific pathological inclusions within individual neurons. Data from this patient demonstrate that severe focal neurodegeneration can occur in the absence of TDP-43 inclusions. At the same time, her findings suggest that while no single *C9orf72*-specific pathological feature is sufficient to produce regional degeneration, some combined burden of features within individual neurons may confer toxicity or overwhelm homeostatic controls. Case 2 afforded an unprecedented opportunity to examine brain MRI scans and brain tissues from the presymptomatic and symptomatic stages in the same patient. Her findings demonstrate that mild brain volume deficits, RNA foci, and dipeptide repeat protein inclusions can emerge years prior to FTD symptoms and TDP-43 aggregation. Although these ideas have been suggested by previous cross-sectional brain imaging (Rohrer *et al.*, 2015) and pathological (Proudfoot *et al.*, 2014; Baborie *et al.*, 2015) studies, the serial MRI and neuropathological data from Case 2 provide the first definitive evidence regarding the pathological sequence in *C9orf72*-FTD.

Distinctive clinical features: spells, seizures, and the new 'thalamic dementia'

The patients described here had symptoms within the broad FTD spectrum. Behavioural deficits predominated in both but in Case 2 were accompanied by language, memory, and visuospatial impairment. Both patients exhibited a variety of peculiar spells without an electroencephalographic correlate. Spells in Case 1 consisted of altered consciousness, panic, and/or stereotyped behaviours, incapacitating her for hours at a time. Given her pattern of focal atrophy, we hypothesize that these periods of altered awareness reflected perturbed thalamo-cingulo-insular oscillations normally generated by the medial pulvinar thalamus, an emerging major epicentre of *C9orf72* disease (Lee *et al.*, 2014; Rohrer *et al.*, 2015). In past decades, this patient might have been diagnosed with so-called 'thalamic dementia', a term applied when strategic vascular or degenerative thalamic lesions produced profound multi-domain cognitive-behavioural impairment (Abbruzzese *et al.*, 1986; Szirmai *et al.*, 2002). The refractory seizure disorder in Case 2 was most likely due to her childhood head trauma. A recent report, however, described photosensitive seizures in two patients with the *C9orf72* repeat expansion (Janssen *et al.*, 2016), raising the possibility that RNA foci, dipeptide repeat protein inclusions, or other *C9orf72*-associated abnormalities embedded in Case 2's temporal lobe seizure focus may have exacerbated her epilepsy.

Dipeptide inclusions and RNA foci can occur prior to the onset of FTD symptoms

Previous reports describing *C9orf72* mutation carriers who died before their degenerative syndrome reached end-stage have suggested that dipeptide repeat protein inclusions may

emerge early, at a time when TDP-43 aggregation is absent (Proudfoot *et al.*, 2014; Baborie *et al.*, 2015). These cross-sectional post-mortem studies, however, provide only indirect evidence about an individual patient's possible progression. Here, in Case 2, neuroimaging and brain tissue were available during both the presymptomatic and symptomatic stages. Brain MRI obtained 15 years prior to symptom onset showed grey matter deficits, which remained stable over a 10-year interval but had worsened upon re-imaging during the symptomatic phase. The presymptomatic volume reductions in dorsal frontoparietal regions could have reflected her history of head trauma or seizures, but, in our view, they more likely reflect an early degenerative or neurodevelopmental consequence of the *C9orf72* expansion. Consistent with this hypothesis, a recent report showed brain volume deficits, including the cortex and thalamus, in *C9orf72* expansion carriers 25 years prior to expected symptom onset (Rohrer *et al.*, 2015). Pathological examination of Case 2 surgical tissue, resected 5 years prior to symptom onset, showed RNA foci and dipeptide repeat protein inclusions, proving that *C9orf72* expansion-specific inclusions can emerge during the presymptomatic phase in a patient who will later manifest *C9orf72*-FTD and FTLD-TDP. Although the surgical tissue was resected only 5 years prior to FTD symptom onset, we speculate that the *C9orf72*-specific phenomena began much earlier in life, exerting a subtle impact on brain structure and function. Consistent with this idea, a previous study found GA dipeptide repeat protein inclusions in the brain of a 26-year-old *C9orf72* mutation carrier with severe developmental disability who died prematurely due to a pulmonary embolism (Proudfoot *et al.*, 2014).

In the surgically resected tissue from Case 2, TDP-43 inclusion pathology was all but absent, whereas at autopsy this patient showed abundant TDP-43 inclusions. Intriguingly, surgical tissue also contained numerous neurons that lacked normal nuclear TDP-43 in the absence of cytoplasmic inclusions; most often these neurons appeared severely degenerate. Neurons with a similar phenotype were also observed, albeit rarely, in the post-mortem brain. Whether these neurons represent an early *C9orf72*-related pathological transition stage or a consequence of surgery, local tissue hypoxia, or epilepsy remains unclear. If these neurons reflect *C9orf72* disease, nuclear TDP-43 depletion could have resulted from diminished TDP-43 expression or restricted access to the nucleus due to nucleocytoplasmic transport impairment (Freibaum *et al.*, 2015; Jovicic *et al.*, 2015; Zhang *et al.*, 2015). Further work is needed to determine whether loss of nuclear TDP-43 in the absence of a TDP-43 inclusion relates to particular *C9orf72*-specific inclusions, as suggested in a recent study (Cooper-Knock *et al.*, 2015). Moreover, the absence of a proximal somatodendritic TDP-43 inclusion does not rule out an inclusion somewhere in the distal neuron or composed of a TDP-43 species not recognized by the antibodies used here. Overall, however, our findings suggest that, in *C9orf72* expansion carriers, TDP-43 aggregation happens at a later disease stage, downstream to RNA foci, dipeptide repeat protein inclusions, and possibly loss of nuclear TDP-43. Although TDP-43 inclusions could have been present in non-resected brain regions at the time of surgery, it seems reasonable to conclude that, at least in the left temporal lobe, *C9orf72*-specific changes preceded the TDP-43 aggregation that would have emerged, as it did throughout the rest of the brain, had the temporal lobe not been therapeutically resected.

Neurodegeneration without TDP-43 inclusion pathology

The typical comingling of TDP-43 inclusions, RNA foci, and dipeptide repeat protein inclusions makes it difficult to correlate any one feature with neurodegeneration severity. By studying Case 1, who showed such sparse TDP-43 pathology, we were able to better estimate the impact of expansion-specific events on a region-wise basis. Overall, Case 1 showed a paucity of brain-wide neurodegeneration. Antemortem MRI and a post-mortem regional survey converged to show focal neurodegeneration in the mPULV, subgenual anterior cingulate cortex and amygdala. In these affected and other unaffected regions, TDP-43 pathology ranged from scarce to absent, whereas several expansion-specific inclusion types were abundant. Therefore TDP-43 inclusions cannot be necessary for neurodegeneration in all cases, including some with a full-blown *C9orf72*-bvFTD syndrome. This assertion comes with the caveat, however, that TDP-43 dysfunction could still occur in the absence of frank TDP-43 inclusions. Furthermore, viewed from a different perspective, the mild overall neurodegeneration seen in Case 1 could reflect the lack of TDP-43 aggregation. What remains uncertain, however, is whether the bvFTD syndrome in Case 1 reflected strategic neurodegeneration in key cortical and thalamic hubs (Lee *et al.*, 2014) or more widespread neuronal dysfunction. In either case, the resulting clinical impairment appears to be best ascribed to *C9orf72*-specific pathological changes, as TDP-43 inclusions were all but absent. Development of the bvFTD syndrome based on neuronal dysfunction alone, as suggested in some previous studies (Boeve *et al.*, 2012; Khan *et al.*, 2012), raises important questions about the physiological basis of that dysfunction; determining this basis could suggest novel therapeutic approaches.

What is the impact of *C9orf72*-specific pathological features?

The cellular toxicity of RNA foci and dipeptide repeat proteins has been well-documented (Donnelly *et al.*, 2013; Lee *et al.*, 2013; Kwon *et al.*, 2014; Mizielinska *et al.*, 2014; Wen *et al.*, 2014), but intense debate surrounds which of these pathological lesions is most relevant to human

disease. In Case 1, sense and antisense RNA foci and GP, GA, and GR dipeptide repeat protein inclusions were abundant, even in regions that lacked neurodegeneration. Therefore, it seems unlikely that any of these inclusion types is sufficient to produce neurodegeneration on its own. By examining multiple features simultaneously, however, we found that a diversity of lesions within individual neurons could be one mechanism driving selective neuronal vulnerability. In both cases, most neurons in the mPULV had more than one type of expansion-specific lesion, and many neurons showed all three features we studied. Larger, more comprehensive studies are needed to explore the link between lesion multiplicity and toxicity within the thalamus and other vulnerable regions and cell types.

RNA foci and dipeptide repeat protein neuronal intranuclear inclusions are often associated with the nucleolus

The nucleolus is essential for ribosomal biogenesis and plays an important role in neuronal growth and long-term homeostasis (Hetman and Pietrzak, 2012). In the course of this study, we observed that RNA foci and dipeptide repeat protein inclusions are found in close association with the nucleolus. In a previous study of *C9orf72*-FTD/ALS, sense foci were shown to co-localize with the nucleolar protein nucleolin (Haeusler *et al.*, 2014). Our analysis, however, revealed that often multiple antisense foci and rarely sense foci were found abutting the outer borders of the nucleolus, where they exhibit a characteristic 'nucleolar studding' pattern around but not within the nucleolus. Likewise, dipeptide repeat protein inclusions within the nucleus were often juxtanucleolar, consistent with recent findings (Schludi *et al.*, 2015). It remains unclear how these inclusions interact with the nucleolar structure and whether this interaction leads to nucleolar dysfunction.

Conclusion

The cases presented here provide critical insights into *C9orf72* expansion-related FTD. RNA foci, dipeptide inclusions and brain atrophy co-exist 5 to 15 years prior to clinical onset, arguing for a long prodromal phase that may involve TDP-43 loss of function or dysfunction. TDP-43 aggregation, on the other hand, arises downstream to these features and may play a key role in driving or reflecting the aggressive neurodegenerative phase associated with symptom onset. These conclusions notwithstanding, mild and focal neurodegeneration can occur in the absence of TDP-43 pathology, and further work is needed to understand mechanisms driving this 'TDP-43 inclusion-independent' degeneration and dysfunction. Neurons in vulnerable regions can have multiple pathological lesion types, and lesion multiplicity or diversity could represent key drivers of toxicity. Early therapeutic interventions targeting expansion-specific inclusion formation may therefore play a role in preventing or delaying symptom onset.

Acknowledgements

We thank participants and their families for their invaluable contributions to neurodegeneration research.

Funding

This work was supported by the NIH/National Institute of Aging (P50 AG023501 to B.L.M. and W.W.S., P01 AG019724 to B.L.M. and W.W.S., P50AG016574 to L.P., and P30AG044281 to R.C.G.) and Consortium for Frontotemporal Dementia Research. This work was supported by the National Institutes of Health/National Institute of Neurological Disorders and Stroke [K23NS095755 (R.C.G.), R21NS089979 (T.F.G.), R21NS084528 (L.P.), R01NS088689 (L.P.), R01NS063964 (L.P.); R01NS077402 (L.P.); P01NS084974 (L.P.)], National Institute of Environmental Health Services [R01ES20395 (L.P.)], and the ALS Association (T.F.G., L.P.). Antibodies generated by L.P. and T.F.G. used in this study have been licensed to commercial entities.

Supplementary material

Supplementary material is available at *Brain* online.

References

Abbruzzese G, Arata L, Bino G, Dall'Agata D, Leonardi A. Thalamic dementia: report of a case with unusual lesion location. Ital J Neurol Sci 1986; 7: 155–9.

Ash PE, Bieniek KF, Gendron TF, Caulfield T, Lin WL, Dejesus-Hernandez M, et al. Unconventional translation of C9ORF72 GGGGCC expansion generates insoluble polypeptides specific to c9FTD/ALS. Neuron 2013; 77: 639–46.

Baborie A, Griffiths TD, Jaros E, Perry R, McKeith IG, Burn DJ, et al. Accumulation of dipeptide repeat proteins predates that of TDP-43 in frontotemporal lobar degeneration associated with hexanucleotide repeat expansions in C9ORF72 gene. Neuropathol Appl Neurobiol 2015; 41: 601–12.

Boeve BF, Boylan KB, Graff-Radford NR, DeJesus-Hernandez M, Knopman DS, Pedraza O, et al. Characterization of frontotemporal dementia and/or amyotrophic lateral sclerosis associated with the GGGGCC repeat expansion in C9ORF72. Brain 2012; 135(Pt 3): 765–83.

Cooper-Knock J, Higginbottom A, Stopford MJ, Highley JR, Ince PG, Wharton SB, et al. Antisense RNA foci in the motor neurons of C9ORF72-ALS patients are associated with TDP-43 proteinopathy. Acta Neuropathol 2015; 130: 63–75.

DeJesus-Hernandez M, Mackenzie IR, Boeve BF, Boxer AL, Baker M, Rutherford NJ, et al. Expanded GGGGCC hexanucleotide repeat in noncoding region of C9ORF72 causes chromosome 9p-linked FTD and ALS. Neuron 2011; 72: 245–56.

Donnelly CJ, Zhang PW, Pham JT, Haeusler AR, Mistry NA, Vidensky S, et al. RNA toxicity from the ALS/FTD C9ORF72 expansion is mitigated by antisense intervention. Neuron 2013; 80: 415–28.

Freibaum BD, Lu Y, Lopez-Gonzalez R, Kim NC, Almeida S, Lee KH, et al. GGGGCC repeat expansion in C9orf72 compromises nucleocytoplasmic transport. Nature 2015; 525: 129–33.

Gendron TF, Bieniek KF, Zhang YJ, Jansen-West K, Ash PE, Caulfield T, et al. Antisense transcripts of the expanded C9ORF72 hexanucleotide repeat form nuclear RNA foci and undergo repeat-associated non-ATG translation in c9FTD/ALS. Acta Neuropathol 2013; 126: 829–44.

Gijselinck I, Van Langenhove T, van der Zee J, Sleegers K, Philtjens S, Kleinberger G, et al. A C9orf72 promoter repeat expansion in a Flanders-Belgian cohort with disorders of the frontotemporal lobar degeneration-amyotrophic lateral sclerosis spectrum: a gene identification study. Lancet Neurol 2012; 11: 54–65.

Haeusler AR, Donnelly CJ, Periz G, Simko EA, Shaw PG, Kim MS, et al. C9orf72 nucleotide repeat structures initiate molecular cascades of disease. Nature 2014; 507: 195–200.

Hetman M, Pietrzak M. Emerging roles of the neuronal nucleolus. Trends Neurosci 2012; 35: 305–14.

Janssen P, Houben M, Hoff E. Photosensitivity in a patient with C9orf72 repeat expansion. Amyotroph Lateral Scler Frontotemporal Degener 2016; 17: 266–9.

Jovicic A, Mertens J, Boeynaems S, Bogaert E, Chai N, Yamada SB, et al. Modifiers of C9orf72 dipeptide repeat toxicity connect nucleocytoplasmic transport defects to FTD/ALS. Nat Neurosci 2015; 18: 1226–9.

Karageorgiou E, Miller BL. Frontotemporal lobar degeneration: a clinical approach. Semin Neurol 2014; 34: 189–201.

Khan BK, Yokoyama JS, Takada LT, Sha SJ, Rutherford NJ, Fong JC, et al. Atypical, slowly progressive behavioural variant frontotemporal dementia associated with C9ORF72 hexanucleotide expansion. J Neurol Neurosurg Psychiatry 2012; 83: 358–64.

Kwon I, Xiang S, Kato M, Wu L, Theodoropoulos P, Wang T, et al. Poly-dipeptides encoded by the C9orf72 repeats bind nucleoli, impede RNA biogenesis, and kill cells. Science 2014; 345: 1139–45.

Lee SE, Khazenzon AM, Trujillo AJ, Guo CC, Yokoyama JS, Sha SJ, et al. Altered network connectivity in frontotemporal dementia with C9orf72 hexanucleotide repeat expansion. Brain 2014; 137(Pt 11): 3047–60.

Lee YB, Chen HJ, Peres JN, Gomez-Deza J, Attig J, Stalekar M, et al. Hexanucleotide repeats in ALS/FTD form length-dependent RNA foci, sequester RNA binding proteins, and are neurotoxic. Cell Rep 2013; 5: 1178–86.

Mackenzie IR, Arzberger T, Kremmer E, Troost D, Lorenzl S, Mori K, et al. Dipeptide repeat protein pathology in C9ORF72 mutation cases: clinico-pathological correlations. Acta Neuropathol 2013; 126: 859–79.

Mackenzie IR, Frick P, Grasser FA, Gendron TF, Petrucelli L, Cashman NR, et al. Quantitative analysis and clinico-pathological correlations of different dipeptide repeat protein pathologies in C9ORF72 mutation carriers. Acta Neuropathol 2015; 130: 845–61.

Mahoney CJ, Beck J, Rohrer JD, Lashley T, Mok K, Shakespeare T, et al. Frontotemporal dementia with the C9ORF72 hexanucleotide repeat expansion: clinical, neuroanatomical and neuropathological features. Brain 2012; 135(Pt 3): 736–50.

Mann DM, Rollinson S, Robinson A, Bennion Callister J, Thompson JC, Snowden JS, et al. Dipeptide repeat proteins are present in the p62 positive inclusions in patients with frontotemporal lobar degeneration and motor neurone disease associated with expansions in C9ORF72. Acta Neuropathol Commun 2013; 1: 68.

Miki Y, Mori F, Tanji K, Kurotaki H, Kakita A, Takahashi H, et al. An autopsy case of incipient Pick's disease: immunohistochemical profile of early-stage Pick body formation. Neuropathology 2014; 34: 386–91.

Mizielinska S, Gronke S, Niccoli T, Ridler CE, Clayton EL, Devoy A, et al. C9orf72 repeat expansions cause neurodegeneration in Drosophila through arginine-rich proteins. Science 2014; 345: 1192–4.

Mizielinska S, Lashley T, Norona FE, Clayton EL, Ridler CE, Fratta P, et al. C9orf72 frontotemporal lobar degeneration is characterised by frequent neuronal sense and antisense RNA foci. Acta Neuropathol 2013; 126: 845–57.

Mori K, Lammich S, Mackenzie IR, Forne I, Zilow S, Kretzschmar H, et al. hnRNP A3 binds to GGGGCC repeats and is a constituent of p62-positive/TDP43-negative inclusions in the hippocampus of patients with C9orf72 mutations. Acta neuropathologica 2013a; 125: 413–23.

Mori K, Weng SM, Arzberger T, May S, Rentzsch K, Kremmer E, et al. The C9orf72 GGGGCC repeat is translated into aggregating dipeptide-repeat proteins in FTLD/ALS. Science 2013b; 339: 1335–8.

Proudfoot M, Gutowski NJ, Edbauer D, Hilton DA, Stephens M, Rankin J, et al. Early dipeptide repeat pathology in a frontotemporal dementia kindred with C9ORF72 mutation and intellectual disability. Acta Neuropathol 2014; 127: 451–8.

Renton AE, Majounie E, Waite A, Simon-Sanchez J, Rollinson S, Gibbs JR, et al. A hexanucleotide repeat expansion in C9ORF72 is the cause of chromosome 9p21-linked ALS-FTD. Neuron 2011; 72: 257–68.

Rohrer JD, Nicholas JM, Cash DM, van Swieten J, Dopper E, Jiskoot L, et al. Presymptomatic cognitive and neuroanatomical changes in genetic frontotemporal dementia in the Genetic Frontotemporal dementia Initiative (GENFI) study: a cross-sectional analysis. Lancet Neurol 2015; 14: 253–62.

Sareen D, O'Rourke JG, Meera P, Muhammad AK, Grant S, Simpkinson M, et al. Targeting RNA foci in iPSC–derived motor neurons from ALS patients with a C9ORF72 repeat expansion. Sci Trans Med 2013; 5: 208ra149.

Schludi MH, May S, Grasser FA, Rentzsch K, Kremmer E, Kupper C, et al. Distribution of dipeptide repeat proteins in cellular models and C9orf72 mutation cases suggests link to transcriptional silencing. Acta Neuropathol 2015; 130: 537–55.

Sha SJ, Takada LT, Rankin KP, Yokoyama JS, Rutherford NJ, Fong JC, et al. Frontotemporal dementia due to C9ORF72 mutations: clinical and imaging features. Neurology 2012; 79: 1002–11.

Suhonen NM, Kaivorinne AL, Moilanen V, Bode M, Takalo R, Hanninen T, et al. Slowly progressive frontotemporal lobar degeneration caused by the C9ORF72 repeat expansion: a 20-year follow-up study. Neurocase 2015; 21: 85–9.

Szirmai I, Vastagh I, Szombathelyi E, Kamondi A. Strategic infarcts of the thalamus in vascular dementia. J Neurol Sci 2002; 203-204: 91–7.

Wen X, Tan W, Westergard T, Krishnamurthy K, Markandaiah SS, Shi Y, et al. Antisense proline-arginine RAN dipeptides linked to C9ORF72-ALS/FTD form toxic nuclear aggregates that initiate *in vitro* and *in vivo* neuronal death. Neuron 2014; 84: 1213–25.

Zhang K, Donnelly CJ, Haeusler AR, Grima JC, Machamer JB, Steinwald P, et al. The C9orf72 repeat expansion disrupts nucleocytoplasmic transport. Nature 2015; 525: 56–61.

Zhang YJ, Jansen-West K, Xu YF, Gendron TF, Bieniek KF, Lin WL, et al. Aggregation-prone c9FTD/ALS poly(GA) RAN-translated proteins cause neurotoxicity by inducing ER stress. Acta Neuropathol 2014; 128: 505–24.

Zu T, Gibbens B, Doty NS, Gomes-Pereira M, Huguet A, Stone MD, et al. Non-ATG-initiated translation directed by microsatellite expansions. Proc Natl Acad Sci USA 2011; 108: 260–5.

Zu T, Liu Y, Banez-Coronel M, Reid T, Pletnikova O, Lewis J, et al. RAN proteins and RNA foci from antisense transcripts in C9ORF72 ALS and frontotemporal dementia. Proc Natl Acad Sci USA 2013; 110: E4968–77.